Multifractal analysis of deep white matter microstructural changes on MRI in relation to early-stage atherosclerosis

Elsevier Editorial System(tm) for NeuroImage

Manuscript Draft

Manuscript Number: NIMG-05-998R2

Title: Multifractal analysis of deep white matter microstructural changes on MRI in relation to early-stage atherosclerosis

Article Type: Regular Article

Section/Category: Methods & Modelling

Keywords:

Corresponding Author: Dr. Tetsuhito Murata,

Corresponding Author's Institution:

First Author: Tetsuya Takahashi, PhD, MD

Order of Authors: Tetsuya Takahashi, PhD, MD; Tetsuhito Murata; Kosuke Narita, MD; Toshihiko Hamada, PhD; Hirotaka Kosaka, PhD, MD; Masao Omori, PhD, MD; Koichi Takahashi, PhD; Hirohiko Kimura, PhD, MD; Haruyoshi Yoshida, PhD, MD; Yuji Wada, PhD,MD

Manuscript Region of Origin:

Abstract: Multifractal analysis based on generalized concepts of fractals has been applied to evaluate biological tissues composed of complex structures. This type of analysis can provide a precise quantitative description of a broad range of heterogeneous phenomena. Previously, we applied multifractal analysis to describe heterogeneity in white matter signal fluctuation on T2-weighted MR images as a new method of texture analysis and established $\Delta\alpha$ as the most suitable index for evaluating white matter structural complexity (Takahashi et al. J. Neurol. Sci., 2004; 225:33-37). Considerable evidence suggests that pathophysiological processes occurring in deep white matter regions may be partly responsible for cognitive deterioration and dementia in elderly subjects. We carried out a multifractal analysis in a group of 36 healthy

elderly subjects who showed no evidence of atherosclerotic risk factors to examine the microstructural changes of the deep white matter on T2-weighted MR images. We also performed conventional texture analysis, i.e., determined the standard deviation of signal intensity divided by mean signal intensity (SD/MSI) for comparison with multifractal analysis. Next, we examined the association between the findings of these two types of texture analysis and the ultrasonographically measured intima-media thickness (IMT) of the carotid arteries, a reliable indicator of early carotid atherosclerosis. The severity of carotid IMT was positively associated with $\Delta\alpha$ in the deep white matter region. In addition, this association remained significant after excluding 12 subjects with visually detectable deep white matter hyperintensities on MR images. However, there was no significant association between the severity of carotid IMT and SD/MSI. These results indicate the potential usefulness of applying multifractal analysis to conventional MR images as a new approach to detect the microstructural changes of apparently normal white matter during the early stages of atherosclerosis.

*** Cover Letter**

Dr. Keith Worsley, Section Editor of "*NeuroImage*"
NeuroImage Editorial Office, Elsevier, Inc.

April 18, 2006

Dr. Keith Worsley:

Attached is our **Re-revised manuscript (No.: NIMG-05-998)** entitled "Multifractal analysis of deep white matter microstructural changes on MRI in relation to early-stage atherosclerosis" by T. Takahashi et al., which we are submitting for publication in the Journal of "*NeuroImage*: to the section on **Original Research Article**".

The comments of the three reviewers have been greatly helpful in allowing us to re-revise our manuscript. We have attempted to address each of the issues raised by the reviewers in a point-by-point response in the attached Responding Letter.

I certify that the manuscript, or parts of it, have not been, and will not be submitted elsewhere for publication.

I certify that all the authors have read the papers and have agreed to having their names listed as authors.

I hope you will give favorable consideration to this revised manuscript. Thank you for your consideration to this re-revised manuscript.

Sincerely,

Tetsuhito Murata, M.D., Ph.D.

Reviewers' comments:

Reviewer #1:

General Comments: In revising the manuscript, the authors have obviously made an effort to address the reviewers' comments, but their revisions fail to address one of the major comments from the original review.

In response to Reviewer 1 Comment, the authors add a calculation of mean signal intensity within the ROI as an alternative texture analysis for comparison to their method. This is hardly adequate as a comparison and few researchers would use it alone for statistical texture mapping. Addition of other first and second order descriptive statistics such as intensity variance, and mean/variance of the absolute gradient would have been more convincing and required relatively little effort. For a truly realistic comparison, wavelet (Jafari-Khouzani), run-length (Xu) or co-occurrence matrix (Kovalev, Kurani) analyses would be recommended.

The question of whether the proposed multi-fractal technique outperforms _comparable_ texture analysis methods has not been addressed in revision, and the manuscript remains weakened by this. I consequently cannot recommend publication.

References:

K. Jafari-Khouzani, H. Soltanian-Zadeh, K. Elisevich, and S. Patel. "Comparison of 2D and 3D wavelet features for tle lateralization." In Proc. of SPIE Medical Imaging 2004: Physiology, Function and Structure from Medical Images, volume 5369, pages 593-601, 2004.

V.A. Kovalev, F. Kruggel, H.-J Gertz, and D.Y. von Cramon. "Three-dimensional texture analysis of MRI brain datasets." IEEE Trans. on Medical Imaging, 20(5):424-433,2001.

A.S. Kurani, D.-H Xu, J.D. Furst, and D.S. Raicu. "Co-occurance matrices for volumetric data." 7th IASTED Int'l Conf on Computer Graphics and Imaging, 2004.

D.-H Xu, A.S. Kurani, J.D. Furst, and D.S. Raicu. "Run-length encoding for volumetric texture." 4th IASTED Int'l Conf on Visualization, Imaging and Image Processing, 2004.

As you pointed out, comparison using the value of the mean signal intensity is inappropriate to show the usefulness of multifractal analysis. In this revised version, we have used the standard deviation of signal intensity divided by the mean signal intensity (SD/MSI) instead of the value of the mean signal intensity. A significant correlation was observed between Delta alpha and SD/MSI, and multiple regression analysis was performed separately for them. As a result, Delta alpha [but not SD/MSI] was a significant predictor for intima-media thickness (IMT). These results suggest that multifractal analysis is more useful than other conventional texture analysis methods for the quantification of MRI signal intensity fluctuations in the white matter associated with early carotid atherosclerosis.

Therefore, in the last paragraph of the Introduction, the following description has been added: “To clarify the utility of multifractal analysis, we additionally calculated the standard deviation of signal intensity divided by the mean signal intensity (SD/MSI) as a conventional type of texture analysis in comparison with multifractal analysis”. In the section of *Conventional texture analysis* (Materials and methods), the following description has also been added: “To compare multifractal analysis with conventional texture analysis, we additionally measured the SD/MSI of the absolute gradient in each ROI using the Scion Image Beta 3 processing application (Scion), in addition to calculating multifractal dimensions.”

In the 3rd paragraph of the Results, the following description has been added: “Since there was a significant correlation between $\Delta\alpha$ and SD/MSI, we conducted multiple regression analysis with IMT for $\Delta\alpha$ and SD/MSI.”

In addition, in the 3rd paragraph of the Discussion, the following description

has been added: “In univariate analysis, there was a significant correlation between Δα and SD/MSI. This correlation may be related to the fact that both parameters are evaluating some aspects of fluctuation of the signal intensity. Note that Δα was found to have a positive significant correlation with IMT in all subjects and in the subgroup of subjects without DWMH for both sides, while SD/MSI had a positive significant correlation with IMT for only the right side (Tables 2 and 5). Furthermore, we demonstrated a strong association between IMT and Δα in multiple regression models independent of age, gender, and BMI (Table 3), while there was no significant association between IMT and SD/MSI (Table 4). These results suggest that Δα more accurately reflects texture fluctuation and is a better predictor of the early stage of atherosclerosis than conventional texture analysis such as SD/MSI.”

Reviewer #2:

As reviewer #2 of the first manuscript I while limit my comments to changes pertaining to the issues I raised at that time.

1) The authors now take advantage of previous publications in order to shorten the description of the multifractal analysis method.

2) Possible effects of B0 field inhomogeneities on <DELTA><alpha> have been addressed in several ways including mention of higher order shimming, parallel imaging, and the measurement of <DELTA><alpha> for an ROI outside the brain. Also, the lack of any significant correlation between the <DELTA><alpha>s of background and white matter ROIs argues against any significant effects of B0 field inhomogeneities.

3) The rational for the location and size of the ROIs is now described in detail.

4) Upon reanalysis log-transformation of IMT and <DELTA><alpha> measures proved to be unnecessary and the graphs have been changed accordingly.

5) Analyses pertaining to possible laterality differences were performed.

6) Although extension of the ROIs over more than one slice was not possible with this particular dataset the sizes of the ROIs was increased to obtain more robust estimates of <DELTA><alpha>.

7) Omissions and typographical errors in the figures have been corrected.

The latest version of this manuscript addresses each of the issues I previously raised. In my opinion this novel technique provides a useful method of assessing early-stage white matter changes and may prove to be a useful diagnostic tool. I look forward to its application to the study of other diseases.

Reviewer #2 did not suggest any further revisions.

Reviewer #3:

The authors have applied multifractal analysis methods to investigate textural differences in image intensities as a function of atherosclerotic risks. The fractal measurements do appear to be correlated with intima-media thickness (IMT) as measured by ultrasound. This appears to be an interesting observation as IMT is probably one of the better predictors of sub-clinical atherosclerotic disease.

This is a revised paper and the authors appear to have addressed many of the concerns raised in the initial review. I do have some minor comments and suggestions, but overall this is an interesting and provocative paper, which illustrates that textural features in the images may also be important.

The first concern that I have is with respect to the other supposed measure of texture, which is the mean signal intensity. This has two problems. First, I am not convinced that the mean signal is a measure of texture. I suppose it could be an attribute, but texture is about describing how the signal is varying over the region. The second issue with the

mean intensity is that the data is somehow normalized to a 256-point range with CSF at the top and zero signal at the bottom. How consistent is this sort of normalization? The signal will fluctuate within CSF so how does one set the upper value? Also, there may be problems with dynamic range after setting the maximum value to a relatively small value like 256. While I am not an expert in texture analysis, it would seem that a more appropriate measure would be the standard deviation divided by the mean signal. Of course, this does not describe the spatial scales of the signal fluctuations, but would give information about how the amount of fluctuation in the region. It would seem to be a better measure than just the mean intensity and would obviate the need for intensity normalization. I would imagine that there are Fourier power spectral analysis methods that could be used to relate variations to spatial frequencies in the region, but I'm not convinced that this is essential to study in this paper.

The first reviewer also raised a point that was not adequately addressed about the effects of field inhomogeneities. Unfortunately, the reviewer posed these fluctuations as arising from B0, which is probably not a large effect. The stronger effect will arise from the inhomogeneities of the RF (B1) field and coil sensitivity. In other words, what are the effects of the spatial variations in the coil RF excitation and receiver sensitivity? If somehow these could be estimated and removed prior to the multifractal analysis, that would be preferable although I would imagine over a large sample these inhomogeneity effects will be randomly distributed across the groups. Regardless, it should be discussed as a source of error.

I respectfully disagree with the second reviewer's comment that the text describing the multifractal analysis method has been described elsewhere and should be removed. This is not a standard image analysis approach and the original description was not overly long.

Comment 1. Inappropriateness of the value of mean signal intensity as conventional texture analysis for comparison with multifractal analysis

As you pointed out, multifractal analysis quantifies how the signal varies over the region, and therefore, the use of the value of the mean signal intensity as the other supposed measure of texture for comparison in our previous version was inappropriate. In the present version, according to your suggestion, the standard deviation of signal intensity divided by mean signal intensity (SD/MSI) has been used instead of the value of the mean signal intensity. A significant correlation was observed between Delta alpha and SD/MSI. This correlation may be associated with the fact that both parameters are evaluating some aspects of fluctuation of the signal intensity. In addition, multiple regression analysis was performed separately for Delta alpha and SD/MSI. As a result, Delta alpha [but not SD/MSI] was a significant predictor for intima-media thickness (IMT). These results suggest that multifractal analysis is more useful than other conventional texture analysis methods for the quantitative evaluation of fluctuations of MRI signal intensity in the white matter associated with early carotid atherosclerosis. In addition, as you suggested, the evaluation of other texture analysis methods such as Fourier power spectral analysis methods may also be necessary in the future.

Therefore, in the last paragraph of the Introduction, the following description has been added: “To clarify the utility of multifractal analysis, we additionally calculated the standard deviation of signal intensity divided by the mean signal intensity (SD/MSI) as a conventional type of texture analysis in comparison with multifractal analysis”. In the section of *Conventional texture analysis* (Materials and methods), the following description has also been added: “To compare multifractal analysis with

conventional texture analysis, we additionally measured the SD/MSI of the absolute gradient in each ROI using the Scion Image Beta 3 processing application (Scion), in addition to calculating multifractal dimensions."

In the 3rd paragraph of the Results, the following description has been added: "Since there was a significant correlation between $\Delta\alpha$ and SD/MSI, we conducted multiple regression analysis with IMT for $\Delta\alpha$ and SD/MSI."

In addition, in the 3rd paragraph of the Discussion, the following description has been added: "In univariate analysis, there was a significant correlation between $\Delta\alpha$ and SD/MSI. This correlation may be related to the fact that both parameters are evaluating some aspects of fluctuation of the signal intensity. Note that $\Delta\alpha$ was found to have a positive significant correlation with IMT in all subjects and in the subgroup of subjects without DWMH for both sides, while SD/MSI had a positive significant correlation with IMT for only the right side (Tables 2 and 5). Furthermore, we demonstrated a strong association between IMT and $\Delta\alpha$ in multiple regression models independent of age, gender, and BMI (Table 3), while there was no significant association between IMT and SD/MSI (Table 4). These results suggest that $\Delta\alpha$ more accurately reflects texture fluctuation and is a better predictor of the early stage of atherosclerosis than conventional texture analysis such as SD/MSI."

Comment 2. Necessity for and method of 256-point range gray-scale normalization

Since multifractal analysis is a method for the quantitative evaluation of fluctuations, differences in the signal intensity range among individuals present a methodological problem in analysis. Therefore, the signal intensity range on images should be made consistent. In this study, the highest signal intensity that was most commonly distributed in the background air was regarded as maximal densities, the

lowest signal intensity that was most commonly distributed in the CSF was regarded as minimal densities, and signal intensity data were converted into 255-gray scale images.

In the 3rd paragraph of the *Multifractal analysis* section (Materials and methods), the following description has been added: "Since multifractal analysis evaluates the fluctuation of the objects, the difference of intensity range among subjects poses an adverse effect in calculating $\Delta\alpha$. Therefore, MRI signal intensity data were converted into 255-gray scale images (the highest signal intensity which is most commonly distributed in background air as maximal densities and the lowest signal intensity which is most commonly distributed in cerebrospinal fluid as minimal densities) using a Scion Image Beta 3 processing application (Scion)."

Comment 3. Reason for the conversion of MR signal intensity into the 255-gray scale (8 bits)

In the multifractal analysis we performed, no marked difference was observed between the algorithmic Delta alpha value using the 4095-gray scale (12 bits) as raw data and that after conversion into the 255-gray scale (8 bits) for actual analysis. We have used the 255-gray scale for analysis because 12 bits markedly prolongs the time required for analysis, and the present program we developed is difficult to use with the conventional method. However, as you suggested, more detailed information can be obtained with a higher resolution. We would like to improve the program so that more detailed data analysis can be performed in the future.

Comment 4. Influences of inhomogeneities of the RF (B1) field and coil sensitivity on multifractal analysis

As you suggested, the influences of the inhomogeneities of the RF (B1) field

and coil sensitivity on multifractal analysis should be evaluated. However, the accurate evaluation of their influences on multifractal analysis is very difficult. We previously reported a significant difference in the Delta alpha value in the white matter between healthy young subjects and healthy elderly subjects under the same MRI conditions. This difference supports the notion that multifractal analysis reflects the fluctuation of the white matter tissue itself (e.g., age-related changes in $\Delta\alpha$) irrespective of the inhomogeneities of the RF field and coil sensitivity.

Therefore, the following description has been added to the section of *Accuracy and sensitivity assessment of multifractal analysis* (Materials and methods): "As other possible sources of error, effects of the inhomogeneities of the RF field and coil sensitivity must be taken into account for multifractal analysis. Previously, we found a significant difference in $\Delta\alpha$ between healthy young subjects and healthy elderly subjects under the same MRI conditions (Takahashi et al., 2004). This difference supports the reflection of the fluctuation of the white matter tissue itself (e.g., age-related changes in $\Delta\alpha$) by multifractal analysis irrespective of the inhomogeneities of the RF field and coil sensitivity."

References:

Takahashi, T., Murata, T., Omori, M., Kosaka, H., Takahashi, K., Yonekura, Y., Wada, Y., 2004. Quantitative evaluation of age-related white matter microstructural changes on MRI by multifractal analysis. J. Neurol. Sci. 225, 33–37.

Comment 5. Description of the multifractal analysis method

Thank you for your valuable suggestion. In our previous version, we made efforts to shorten our text by omitting equations and principles associated with multifractal analysis by citing previous references. However, in the present version,

according to your suggestions, we have described these equations and principle in detail (in the 1st paragraph of the *Multifractal analysis* section of the Materials and methods).

Multifractal analysis of deep white matter microstructural changes on MRI in relation to early-stage atherosclerosis

Tetsuya Takahashi,[a] Tetsuhito Murata,[a,*] Kosuke Narita,[a] Toshihiko Hamada,[b] Hirotaka Kosaka,[a] Masao Omori,[a] Koichi Takahashi,[c] Hirohiko Kimura,[d] Haruyoshi Yoshida,[b] Yuji Wada[a]

[a]Department of Neuropsychiatry, Faculty of Medical Sciences, University of Fukui, Fukui 910-1193, Japan

[b]Department of Clinical and Laboratory Science, Faculty of Medical Sciences, University of Fukui, Fukui 910-1193, Japan

[c]Department of Informatics, Faculty of Science and Engineering, Kinki University, Higashi-Osaka, Japan

[d]Department of Radiology, Faculty of Medical Sciences, University of Fukui, Fukui 910-1193, Japan

*Corresponding author. Department of Neuropsychiatry, Faculty of Medical Sciences, University of Fukui, 23-3 Shimoaizuki, Matsuoka-cho, Yoshida-gun, Fukui 910-1193, Japan. Fax: +81 776 61 8136

E-mail address: tmurata@fmsrsa.fukui-med.ac.jp (T. Murata).

Abstract

Multifractal analysis based on generalized concepts of fractals has been applied to evaluate biological tissues composed of complex structures. This type of analysis can provide a precise quantitative description of a broad range of heterogeneous phenomena. Previously, we applied multifractal analysis to describe heterogeneity in white matter signal fluctuation on T2-weighted MR images as a new method of texture analysis and established $\Delta\alpha$ as the most suitable index for evaluating white matter structural complexity (Takahashi et al. J. Neurol. Sci., 2004; 225:33–37). Considerable evidence suggests that pathophysiological processes occurring in deep white matter regions may be partly responsible for cognitive deterioration and dementia in elderly subjects. We carried out a multifractal analysis in a group of 36 healthy elderly subjects who showed no evidence of atherosclerotic risk factors to examine the microstructural changes of the deep white matter on T2-weighted MR images. We also performed conventional texture analysis, i.e., determined the standard deviation of signal intensity divided by mean signal intensity (SD/MSI) for comparison with multifractal analysis. Next, we examined the association between the findings of these two types of texture analysis and the ultrasonographically measured intima-media thickness (IMT) of the carotid arteries, a reliable indicator of early carotid atherosclerosis. The severity of carotid IMT was positively associated with $\Delta\alpha$ in the deep white matter region. In addition, this association remained significant after excluding 12 subjects with visually detectable deep white matter hyperintensities on MR images. However, there was no significant association between the severity of carotid IMT and SD/MSI. These results indicate the potential usefulness of applying multifractal analysis to conventional MR

images as a new approach to detect the microstructural changes of apparently normal white matter during the early stages of atherosclerosis.

Keywords: Texture analysis; Multifractal; T2-weighted MRI; Deep white matter; Intima-media thickness; Atherosclerosis

Introduction

Considerable evidence has recently suggested that pathophysiological processes in the white matter regions may partly account for a number of brain dysfunctions in elderly subjects. This white matter deterioration may play an important role in clinical deficits such as age-related cognitive decline, geriatric depression, or dementia (Gunning-Dixon and Raz, 2003; Valenzuela et al., 2000). Therefore, the deterioration of white matter should be evaluated at the earliest possible stage. T2-weighted MRI has demonstrated a high prevalence of white matter changes with aging. These changes frequently occur in deep white matter, i.e., the terminal zone of the penetrating medullary arteries (Kirkpatrick and Hayman, 1987; van Swieten et al., 1991), and they are reflected in MR signals such as deep white matter hyperintensities (DWMHs). DWMHs are related to standard risk factors for cardiovascular diseases and are believed to be a consequence of cerebrovascular disease (Bots et al., 1993; Fazekas et al., 1988; Manolio et al., 1994).

Another method, ultrasonographic measurement of the intima-media thickness (IMT) of carotid arteries, is reported to be a reliable indicator of the early stage of atherosclerosis (Allan et al., 1997; Burke et al., 1995). Given that the carotid arteries provide most of the blood supply to the brain, carotid atherosclerotic changes of IMT may be associated with a higher risk of cerebrovascular disease (Manolio et al., 1999; Touboul et al., 2000) and are regarded as a robust predictor of stroke (Cao et al., 2003; O'Leary et al., 1999). Several studies have also elucidated the relationship between IMT and visible white matter hyperintensities on MRI (Manolio et al., 1999; Pico et al., 2002).

The analysis of texture parameters is a useful way of increasing the information obtainable from MR signal changes. Various types of texture analysis have been applied for the delineation and separation of tissue alterations (Castellano et al., 2004). However, the current clinical diagnosis of white matter degeneration on T2-weighted MR images still depends on visual rating scales due to the lack of appropriate measurement tools. Accordingly, there is demand for a more sophisticated method that can provide a better description of pathological changes on MR images, especially in the early stage. Fractals, proposed by Mandelbrot (1983), are characterized by self-similar structures, and fractal theory provides a new scale of nonlinearity. Various physical phenomena such as the growth of cancers and arterial and bronchial trees show the features of fractals, and fractal theory has already provided clinically useful information to differentiate pathological tissue from healthy tissue (Baish and Jain, 2000; Mauroy et al., 2004; Zamir, 1999). The application of fractal theory to the neuroimaging field has also provided novel and useful information in clinical medicine (Kiselev et al., 2003; Yoshikawa et al., 2003a, 2003b). In contrast to simple fractals, the concept of "multifractal phenomena" holds that different regions of an object have different local fractal properties that quantify local singular behavior (Halsey et al., 1986). To describe these local fractal properties, Halsey et al. (1986) introduced α, the so-called Lipschitz-Hölder index (or the strength of singularity), and the multifractal spectrum $f(\alpha)$. Multifractal scaling provides a quantitative description of a broad range of heterogeneous complex phenomena that are impossible to evaluate using simple fractals (Ivanov et al., 1999; Shimizu et al., 2004; Stanley et al., 1999).

Our previous study showed that index $\Delta\alpha$ (established as the most suitable index of heterogeneity in Takahashi et al. (2001)), in apparently normal deep white

matter frontal regions on T2-MRI, reached significantly higher levels in elderly subjects than in young subjects and was correlated with cognitive decline in elderly subjects (Takahashi et al., 2004). Yet, the underlying pathogenesis behind these changes in the deep white matter in elderly subjects remains obscure. In this study we carried out a multifractal analysis to examine the microstructural changes of the deep white matter in apparently normal T2-weighted MR images in elderly subjects who showed no evidence of atherosclerotic risk factors. To clarify the utility of multifractal analysis, we additionally calculated the standard deviation of signal intensity divided by the mean signal intensity (SD/MSI) as a conventional type of texture analysis in comparison with multifractal analysis. We also sought to identify the pathogenesis of these changes with special reference to ultrasonographic measurements of carotid artery IMT, a reliable indicator of the early stage of atherosclerosis. Last, we re-examined the relationships among these changes in view of the coexistence of DWMH.

Materials and methods

Subjects and study design

Forty-three healthy elderly subjects were recruited from the general population in Fukui prefecture, Japan; a brochure described the following exclusion criteria: history of major atherosclerotic risk factors (such as hypertension, hypercholesterolemia, diabetes mellitus, coronary artery disease, congestive heart failure, and hemodynamically significant valvular disease), history of psychiatric treatment, chronic alcoholism, smoking, obesity with a body mass index (BMI) above 26, and the continuous administration of drugs. All female subjects were postmenopausal. Of the 43 volunteers, 7 were excluded due to the confined space for setting the ROI and a high

prevalence of DWMH, which precluded subsequent multifractal analysis (as described in the section on *"Multifractal analysis"*). Finally, 36 volunteers (23 males aged 52–72 (mean: 61.0 ± 4.7 years) and 13 females aged 55–70 (mean: 60.9 ± 4.1 years)) were included in the study. All subjects gave written informed consent.

The protocol of this study was approved by the ethics committee of our university. Data from each examination were analyzed independently by different clinical technologists, radiologists or psychiatrists who were blinded to the data collected in other examinations.

Multifractal analysis

The idea of the multifractal is a generalized concept based on Mandelbrot's fractal (Halsey et al., 1986; Mandelbrot, 1983). Details of multifractal analysis are provided elsewhere (Takahashi et al., 2001, 2004). Briefly, after dividing an image into squares with sides having length r, we define a probability density for each square box as $p_i = N_i / N$, where N_i is the density at the i-th box and $N = \sum_i N_i$ is the total density of the image. The density of the images with nonlinear structures fluctuates and reveals fractality. To estimate this fractality, Halsey et al. (1986) proposed the q-th moment of probability density to be $\sum_i p_i^q$, a generalization of the conventional partition function $\sum_i p_i$. When the probability scales as $p_i \propto r^{\alpha i}$, α_i represents a local fractal dimension at the i-th box. Halsey et al. (1986) have defined a mass index $\tau(q)$ by

$$\lim_{r \to 0} (\sum_i p_i^q / r^{\tau(q)}) = 1.$$

$\tau(q)$ relates to the so-called generalized fractal dimension $D(q)$ (Grassberger, 1983; Hentschel and Procaccia, 1983) as $\tau(q) = (q-1)\,D(q)$. By mathematical manipulation (Halsey et al., 1986), we obtain

$$\alpha(q) = d\tau(q)/dq.$$

$\alpha(q)$, the Lipschitz-Hölder index (or the strength of singularity after Halsey et al. (1986)), represents the local dimension. For the set with a constant $\alpha(q)$ on the image, Mandelbrot's fractal dimension (the capacity dimension) is given as (Halsey et al., 1986)

$$f(\alpha(q)) = q\,\alpha(q) - \tau(q).$$

Analogies between multifractal theory and classical thermodynamics can be drawn as follows. q corresponds to inverse temperature, $\alpha(q)$ to energy, $f(\alpha(q))$ to entropy, and $\tau(q)/q$ to free energy.

Actually, $f(\alpha)$ is the smooth concave function of α, typical examples of which are shown in Fig. 1. Theoretically, $\alpha(q)$ with large positive q values corresponds to the most concentrated regions (low intensity regions of the image, i.e., dark regions) and $\alpha(q)$ with large negative q values corresponds to the most rarefied regions (high intensity regions of the image, i.e., white regions). In addition, the width of both ends of the $f(\alpha)$ spectrum reveal the image's heterogeneity. Since $\alpha(q)$ tended to be constant at $|q| > 20$ in this study, the width between the $\alpha(q)$ value at $q = -20$ (the right end of the $f(\alpha)$ spectrum in Fig. 1) and the $\alpha(q)$ value at $q = +20$ (the left end of the $f(\alpha)$ spectrum in Fig. 1) was defined as $\Delta\alpha$ (the width of both ends of the $f(\alpha)$ spectrum in Fig. 1). Our previous studies showed that $\Delta\alpha$ is the most suitable multifractal index of heterogeneity on MRI (Takahashi et al., 2001, 2004).

Brain MRI was performed using a General Electric 1.5-Tesla Signa system. Axial T2-weighted images (TR = 3000 ms, TE = 80 ms) were obtained parallel to the orbitomeatal line. The slice thickness was 5 mm and the matrix size was 512 × 512. No spatial filter was used prior to multifractal analysis, although the Fermi spatial filter built in the GE MR imaging system was used during reconstruction. Since multifractal analysis evaluates the fluctuation of the objects, the difference of intensity range among subjects poses an adverse effect in calculating $\Delta\alpha$. Therefore, MRI signal intensity data were converted into 255-gray scale images (the highest signal intensity which is most commonly distributed in background air as maximal densities and the lowest signal intensity which is most commonly distributed in cerebrospinal fluid as minimal densities) using a Scion Image Beta 3 processing application (Scion). The "power of 2" box size (i.e., $r = 2^n$) is needed to divide the image to calculate the $f(\alpha)$ spectrum, and an increase in size will theoretically provide more stable results. Previously, we reported the necessity for at least 32 × 32 pixel images to achieve a stable $f(\alpha)$ spectrum according to the size and resolution of the images (Takahashi et al., 2004). In this study, the establishment of ROIs was restricted because we included subjects with DWMH, which must be excluded from the ROI. In the actual analysis, to achieve more robust data, a rectangular ROI of $x \times y$ pixels ($1600 < x \times y < 2000$; $x, y > 32$ pixels) was placed bilaterally in the deep white matter of the frontoparietal region in the vicinity of the lateral ventricles (Figs. 2A and 2B) as the ROI. ROIs were chosen to avoid including the cortex, the ventricles, and the abnormal white matter intensities manually by T.T. and K.N. Since the rectangular ROI consisted of $(x - 32 + 1) \times (y - 32 + 1)$ frames of 32 × 32 pixel images (Fig. 2C with magnification), we performed multifractal analysis to these subframes separately and averaged them all for subsequent analysis.

The interrater reliability (intraclass correlation coefficient), established by two different evaluators (T.T. and K.N.), was $r = 0.813$ for the right $\Delta\alpha$ and $r = 0.912$ for the left $\Delta\alpha$. Prior to calculating the multifractal dimensions, all selected ROIs were visually inspected and determined to be normal (as shown in Figs. 3E1 and 3E2) by an experienced radiologist (H.K.). As a result of setting this condition, however, we had to exclude 7 subjects from further analysis due to restrictions in the establishment of the ROIs (confined space for setting the ROIs and high prevalence of DWMH). The MR signal intensity fluctuations in these ROIs (as shown in Fig. 2C with magnification) of the remaining subjects were quantitatively evaluated by multifractal analysis. The sum of the density of the divided image into the *i*-th square with a side of *r* (maximum was 32 pixels) was regarded as N_i, and the sum of the density of the entire image was regarded as N. The probability density in the *i*-th square was defined as $p_i = N_i/N$ for 1, 2, 4, 8, 16, and 32 pixels (Fig. 2D).

DWMHs were graded to ascertain their conventional macroscopic classifications for hyperintensity on T2-weighted images according to the system of Fazekas (Fazekas et al., 1988) (grade 0 = absent; grade 1 = punctuate foci; grade 2 = beginning confluence of foci; grade 3 = large confluent areas). The 36 subjects were classified as follows: grade 0 (24), 1 (10), 2 (2), or 3 (0) by a skilled radiologist (H.K.). We also divided the subjects into two groups, grade 0 and grades 1–3, due to the small numbers of DWMHs classified specifically as grade 2 or 3.

Conventional texture analysis

To compare multifractal analysis with conventional texture analysis, we additionally measured the SD/MSI of the absolute gradient in each ROI using the Scion

Image Beta 3 processing application (Scion), in addition to calculating multifractal dimensions.

Carotid B-mode ultrasonography

Carotid B-mode ultrasonography was performed using a LOGIQ500 MD MR3 (General Electric Medical Systems), and carotid atherosclerosis was examined using an 8.8-MHz wideband transducer. IMT was measured as the distance between the lumen-intima interface and the media-adventitia interface at the far wall on each side in the B-mode image according to the method of Handa et al. (1990).

Biochemical determinations

All subjects underwent venous blood sampling from an antecubital vein in the right arm at about 11:00 a.m. after an overnight and morning fast. Serum concentrations of total cholesterol (TC) were measured by enzymatic determination.

Twenty-four-hour ambulatory blood pressure monitoring (ABPM)

Twenty-four-hour ABPM was performed using an FM-200 (Fukuda Densi Co., Tokyo, Japan). Blood pressure (BP) was measured at 30-min intervals from 6:00 a.m. to 10:00 p.m. and at one-hour intervals from 10:00 p.m. to 6:00 a.m. In this study, 24-hour mean systolic BP was used.

Accuracy and sensitivity assessment of multifractal analysis

To determine whether our method accurately measured multifractal dimensions, we simulated homogeneous images such as simple gray (Fig. 3A) and a

standard fractal object such as Sierpinski's gasket (Figs. 3B1–3 from homogeneous to heterogeneous type) in comparison with theoretical values. Additionally, randomized noise (Fig. 3C), background air, and the averaged image of 10 ROIs with DWMH (Fig. 3D) were calculated. Figs. 3E1 and 3E2 show the images of selected ROIs with high and low $\Delta\alpha$. Simple gray images resulted in $\Delta\alpha$ close to 0, which indicates that they were completely homogeneous (Fig. 3A). Delta α of Sierpinski's gasket was in line with the theoretical value (Fig. 3F); the line indicates the theoretical value, and the dots reveal the actual value. With increasing image fluctuation (from Fig. B1 to B3), the width of both ends of α gradually increases, results in line with the algorithm of multifractals that substantiate the accuracy of our analysis. Moreover, $\Delta\alpha$s of images with DWMH were extremely large (mean: 0.156, SD: 0.023) compared to those of apparently normal white matter (mean: 0.024, SD: 0.007). We also analyzed background air images in all subjects to identify the effect of background activity. We found extremely high values of $\Delta\alpha$ in background air (mean: 0.505, SD: 0.057, close to the value of noise) compared to those of white matter; there was no significant relationship between the $\Delta\alpha$s of background air images and those of the white matter (right side: $r = -0.052$; left side: $r = 0.093$). These results substantiate the irrelevancy of artifacts in applying multifractal analysis to white matter on T2-weighted MRI. As other possible sources of error, effects of the inhomogeneities of the RF field and coil sensitivity must be taken into account for multifractal analysis. Previously, we found a significant difference in $\Delta\alpha$ between healthy young subjects and healthy elderly subjects under the same MRI conditions (Takahashi et al., 2004). This difference supports the reflection of the fluctuation of the

white matter tissue itself (e.g., age-related changes in $\Delta\alpha$) by multifractal analysis irrespective of the inhomogeneities of the RF field and coil sensitivity.

Statistical analysis

Statistical analysis was carried out using SPSS software for Windows version 12 (SPSS Japan Inc., Tokyo, Japan).

Pearson's χ^2 and Student's *t* test were used to compare the distribution of categorized data and continuous data by gender. The paired *t* test was used to test for laterality differences in $\Delta\alpha$, SD/MSI, and IMT. The relationships among $\Delta\alpha$, SD/MSI, IMT, age, gender, BMI, TC, and mean 24-hour systolic BP were explored by simple correlation analysis using Pearson's product-moment correlation coefficient (*r*). The independent IMT predictors were examined in a multiple regression model in which $\Delta\alpha$, SD/MSI, age, gender, and BMI were introduced as independent variables on both sides. We also calculated these univariate analysis and multiple regression models after eliminating the subjects with DWMH. The relationship between $\Delta\alpha$ and IMT was further investigated using one-way ANCOVA across IMT subgroups on both sides separately, divided into approximate groupings of high (18 subjects) and low (18 subjects) IMT values. Age, gender, and BMI were treated as covariates. *P* values < 0.05 were considered statistically significant.

Results

The demographic characteristics, $\Delta\alpha$, SD/MSI, IMT, age, BMI, TC, mean 24-hour systolic BP, and coexistence of DWMH are presented in Table 1. There were

significant differences in right and left SD/MSI and total cholesterol levels between male and female subjects.

The paired *t* test demonstrated no significant laterality differences for $\Delta\alpha$ (P = 0.773), SD/MSI (P = 0.402), or IMT (P = 0.625).

Table 2 represents the Pearson's product-moment correlation among $\Delta\alpha$, SD/MSI, IMT, age, BMI, TC, and mean 24-hour systolic BP in all subjects separately for right and left sides. There were significant correlations between $\Delta\alpha$ and SD/MSI for the right side (r = 0.624, P < 0.001) and left side (r = 0.618, P < 0.001). Correlations between texture analysis and confounding factors were found in $\Delta\alpha$ and IMT (r = 0.515, P < 0.001; open and closed circles in Fig. 4A), SD/MSI and IMT (r = 0.397, P = 0.016), SD/MSI and BMI (r = 0.342, P = 0.041) for the right side, $\Delta\alpha$ and IMT (r = 0.474, P = 0.004; open and closed circles in Fig. 4B), SD/MS and BMI (r = 0.347, P = 0.038) for the left side. Correlations among confounding factors were found in BMI and mean 24-hour systolic BP (r = 0.367, P = 0.028). Since there was a significant correlation between $\Delta\alpha$ and SD/MSI, we conducted multiple regression analysis with IMT for $\Delta\alpha$ and SD/MSI. When variables ($\Delta\alpha$, age, gender, and BMI) were input into multiple regression models, $\Delta\alpha$ was the strongest predictor of IMT for both sides (Table 3). On the other hand, when variables (SD/MSI, age, gender, and BMI) were input into multiple regression models, SD/MSI had no association with IMT (Table 4).

Table 5 represents the Pearson's product-moment correlation among $\Delta\alpha$, SD/MSI, IMT, age, BMI, TC, and mean 24-hour systolic BP, in subjects without DWMH, for the right and left sides separately. There were significant correlations between $\Delta\alpha$ and SD/MSI for the right side (r = 0.592, P = 0.002) and left side (r =

0.454, $P = 0.026$). Correlations between texture analysis and confounding factors were found in $\Delta\alpha$ and IMT ($r = 0.540$, $P = 0.006$; closed circles in Fig. 4A), SD/MSI and BMI ($r = 0.453$, $P = 0.026$) for the right side, and $\Delta\alpha$ and IMT ($r = 0.610$, $P = 0.002$; closed circles in Fig. 4B), and SD/MSI and BMI ($r = 0.412$, $P = 0.042$) for the left side. No significant correlation was found between any combinations of confounding factors. Exclusion of subjects with DWMH did not affect the relationship between $\Delta\alpha$ and IMT in multiple regression models (Table 3).

Fig. 5 shows further evidence of the relationship between $\Delta\alpha$ and IMT. IMT was divided into approximately two subgroups (i.e., low (< 0.84 mm), high (≥ 0.85 mm)), and the means across the subgroups were compared by one-way ANCOVA. One-way ANCOVA with adjustments for age, gender, and BMI indicated that the value of $\Delta\alpha$ was higher in the high-IMT group (right: $F = 6.942$, $P = 0.013$; left: $F = 20.523$, $P < 0.001$). This significant relationship between $\Delta\alpha$ and IMT remained significant after adjustments for age, gender, BMI, TC, and systolic BP (right: $F = 6.523$, $P = 0.016$; left: $F = 19.092$, $P < 0.001$).

Discussion

Previous studies have shown that the properties of T2-weighted MR image signal intensity reflect a broad range of pathological changes, such as demyelination, microtubule deterioration, dilated perivascular spaces, and axonal dilation (Fazekas et al., 1998; Meier-Ruge et al., 1992; Takao et al., 1999). Other studies have demonstrated the roles of these changes in normal aging (Davatzikos and Resnick, 2002; Yamamoto et al., 2005), cognitive function (Gunning-Dixon and Raz, 2003; Ylikoski et al., 1993),

depression (Salloway et al., 1996), and dementia (Varma et al., 2002). These pathological changes in white matter are accompanied by lesions in the small perforating cerebral arteries (Inzitari, 2003; Schmidt et al., 2002, 2004; van Swieten et al., 1991) and are related to the prevalence of peripheral atherosclerosis (Manolio et al., 1999; Pico et al., 2002). Most of these studies were based on visually detectable changes in the white matter (e.g., DWMH), occurring at relatively late stages in the development of pathological changes. These visually detectable changes could be quantified with comparative ease by visual inspection. However, to date no studies have explored the changes that occur at the initial stages (especially in normal-appearing white matter on T2-MRI).

At the initial stages, since these MR signal intensity changes are localized in a very small region associated with cerebral small vessel damage (Inzitari, 2003; Kidwell et al., 2001; Pantoni, 2002; Pugh and Lipsitz, 2002; Schmidt et al., 2002; van Swieten et al., 1991), such minute changes might appear as fluctuations of signal intensity and be difficult to evaluate by conventional methods. Multifractal analysis can provide a good quantitative evaluation of such fluctuations in the signal intensity of the images. Our group previously reported that $\Delta\alpha$ (an index of the heterogeneity of signal intensity) in apparently normal deep white matter regions reached significantly higher levels in elderly subjects than in young subjects and was correlated with executive cognitive decline in the elderly group (Takahashi et al., 2004). However, the underlying causal mechanisms remain obscure.

In the present study we quantitatively examined the MR signal characteristics of the deep white matter region by multifractal analysis in comparison with a conventional method of analysis, i.e., calculation of SD/MSI, and examined the

correlation of these characteristics with ultrasonographic measurements of carotid artery IMT, a reliable indicator of the early stage of atherosclerosis. In univariate analysis, there was a significant correlation between $\Delta\alpha$ and SD/MSI. This correlation may be related to the fact that both parameters are evaluating some aspects of fluctuation of the signal intensity. Note that $\Delta\alpha$ was found to have a positive significant correlation with IMT in all subjects and in the subgroup of subjects without DWMH for both sides, while SD/MSI had a positive significant correlation with IMT for only the right side (Tables 2 and 5). Furthermore, we demonstrated a strong association between IMT and $\Delta\alpha$ in multiple regression models independent of age, gender, and BMI (Table 3), while there was no significant association between IMT and SD/MSI (Table 4). These results suggest that $\Delta\alpha$ more accurately reflects texture fluctuation and is a better predictor of the early stage of atherosclerosis than conventional texture analysis such as SD/MSI. More noteworthy is that the relationship between $\Delta\alpha$ and IMT was observed not only in all subjects but also after eliminating the subjects with DWMH. Thus, detection using the multifractal analysis of microstructural changes in the white matter, specifically changes related to the early stages of atherosclerosis, before the appearance of visible changes on T2-MRI, is clinically significant. IMT is a strong predictor of cerebrovascular disease, including stroke (Cao et al., 2003; Manolio et al., 1999; O'Leary et al., 1999; Touboul et al., 2000). Therefore, this study's quantitative analysis of deep white matter by multifractal analysis is likely to be useful for predicting the occurrence or prognosis of cerebrovascular disease.

Contrary to expectations, there were no significant associations between $\Delta\alpha$ or IMT and confounding factors which were reported to be associated with atherosclerosis

and cerebrovascular damage (Bonithon-Kopp et al., 1996; Bots et al., 1992; Zureik et al., 1999). In addition, very few combinations of confounding factors showed significant correlations. These results were probably related to the stringent exclusion of subjects with atherosclerotic risk factors from this study.

The findings of this study are limited by the following four factors. First, restrictions in the establishment of ROIs must be taken into account. At the present stage, multifractal analysis can only be applied to relatively large ROIs (i.e., 32 × 32 pixel ROIs), and ROI placement is operator dependent. Another consideration for ROI placement is whether the pathological process affects all of the white matter or is localized. Hence, multifractal dimensions could be affected by ROI placement depending on whether the potential pathological process was included in the ROI. To overcome these limitations, we must improve multifractal analysis to permit high resolution and regional analysis. Second, artifacts derived from the MRI technique must be taken into account to enable better descriptions in multifractal analysis. Third, the subjects in the present study were highly restricted due to the exclusive selection of subjects who had no evidence of cardiovascular risk factors. Finally, the small number of subjects needs to be taken into account. Further studies with larger numbers are required to confirm our findings, and longitudinal studies are awaited to corroborate and strengthen our preliminary results. Nevertheless, our findings highlight the potential usefulness of multifractal analysis in MR imaging studies and suggest that this multifractal approach can contribute to identifying the early stages of atherosclerosis through the detection of microstructural changes in apparently normal white matter, which could be crucial in combination with conventional methods.

References

Allan, P.L., Mowbray, P.I., Lee, A.J., Fowkes, F.G., 1997. Relationship between carotid intima-media thickness and symptomatic and asymptomatic peripheral arterial disease: the Edinburgh Artery Study. Stroke 28, 348–353.

Baish, J.W. and Jain, R.K., 2000. Fractals and cancer. Cancer Res. 60, 3683–3688.

Bonithon-Kopp, C., Touboul, P.J., Berr, C., Leroux, C., Mainard, F., Courbon, D., Ducimetiere, P., 1996. Relation of intima-media thickness to atherosclerotic plaques in carotid arteries: the Vascular Aging (EVA) Study. Arterioscler. Thromb. Vasc. Biol. 16, 310–316.

Bots, M.L., Breslau, P.J., Briet, E., de Bruyn, A.M., van Vliet, H.H., van den Ouweland, F.A., de Jong, P.T., Hofman, A., Grobbee, D.E., 1992. Cardiovascular determinants of carotid artery disease: the Rotterdam Elderly Study. Hypertension 19, 717–720.

Bots, M.L., van Swieten, J.C., Breteler, M.M., de Jong, P.T., van Gijn, J., Hofman, A., Grobbee, D.E., 1993. Cerebral white matter lesions and atherosclerosis in the Rotterdam Study. Lancet 341, 1232–1237.

Burke, G.L., Evans, G.W., Riley, W.A., Sharrett, A.R., Howard, G., Barnes, R.W., Rosamond, W., Crow, R.S., Rautaharju, P.M., Heiss, G., 1995. Arterial wall thickness is associated with prevalent cardiovascular disease in middle-aged adults: the Atherosclerosis Risk in Communities (ARIC) Study. Stroke 26, 386–391.

Cao, J.J., Thach, C., Manolio, T.A., Psaty, B.M., Kuller, L.H., Chaves, P.H., Polak, J.F., Sutton-Tyrrell, K., Herrington, D.M., Price, T.R., Cushman, M., 2003. C-reactive protein, carotid intima-media thickness, and incidence of ischemic stroke in the elderly, the Cardiovascular Health Study. Circulation 108, 166–170.

Castellano, G., Bonilha, L., Li, L.M., Cendes, F., 2004. Texture analysis of medical images. Clin. Radiol. 59, 1061–1069.

Davatzikos, C., Resnick, S.M., 2002. Degenerative age changes in white matter connectivity visualized in vivo using magnetic resonance imaging. Cereb. Cortex 12, 767–771.

Fazekas, F., Niederkorn, K., Schmidt, R., Offenbacher, H., Horner, S., Bertha, G., Lechner, H., 1988. White matter signal abnormalities in normal individuals, correlation with carotid ultrasonography, cerebral blood flow measurements, and cerebrovascular risk factors. Stroke 19, 1285–1288.

Fazekas, F., Schmidt, R., Scheltens, P., 1998. Pathophysiologic mechanisms in the development of age-related white matter changes of the brain. Dement. Geriatr. Cogn. Disord. 9 (Suppl. 1), 2–5.

Grassberger, P., 1983. “Generalized dimensions of strange attractors”. Phys. Lett. 97A, 227–230.

Gunning-Dixon, F.M., Raz, N., 2003. Neuroanatomical correlates of selected executive functions in middle-aged and older adults: a prospective MRI study. Neuropsychologia 41, 1929–1941.

Halsey, T.C., Jensen, M.H., Kadanoff, L.P., Procaccia, I., Shraiman, B.I., 1986. Fractal measures and their singularities, the characterization of strange sets. Phys. Rev. A 33, 1141–1151.

Handa, N., Matsumoto, M., Maeda, H., Hougaku, H., Ogawa, S., Fukunaga, R., Yoneda, S., Kimura, K., Kamada, T., 1990. Ultrasonic evaluation of early carotid atherosclerosis. Stroke 21, 1567–1572.

Hentschel, H.G.E. and Procaccia, I., 1983. The infinite number of generalized dimensions of fractals and strange attractor. Physica 8D, 435–444.

Inzitari, D., 2003. Leukoaraiosis, an independent risk factor for stroke? Stroke 34, 2067–2071.

Ivanov, P.C., Amaral, L.A., Goldberger, A.L., Havlin, S., Rosenblum, M.G., Struzik, Z.R., Stanley, H.E., 1999. Multifractality in human heartbeat dynamics. Nature 399, 461–465.

Kidwell, C,S,, el-Saden, S., Livshits, Z., Martin, N.A., Glenn, T.C., Saver, J.L., 2001. Transcranial Doppler pulsatility indices as a measure of diffuse small-vessel disease. J. Neuroimaging 11, 229–235.

Kirkpatrick, J.B., Hayman, L.A., 1987. White-matter lesions in MR imaging of clinically healthy brains of elderly subjects, possible pathologic basis. Radiology 162, 509–511.

Kiselev, V.G., Hahn, K.R., Auer, D.P., 2003. Is the brain cortex a fractal? Neuroimage 20, 1765–1774.

Mandelbrot, B.B., 1983. The Fractal Geometry of Nature. W. H. Freeman, New York.

Manolio, T.A., Kronmal, R.A., Burke, G.L., Poirier, V., O'Leary, D.H., Gardin, J.M., Fried, L.P., Steinberg, E.P., Bryan, R.N., 1994. Magnetic resonance abnormalities and cardiovascular disease in older adults: the Cardiovascular Health Study. Stroke 25, 318–327.

Manolio, T.A., Burke, G.L., O'Leary, D.H., Evans, G., Beauchamp, N., Knepper, L., Ward, B., 1999. Relationships of cerebral MRI findings to ultrasonographic carotid atherosclerosis in older adults: the Cardiovascular Health Study. Arterioscler. Thromb. Vasc. Biol. 19, 356–365.

Mauroy, B., Filoche, M., Weibel, E.R., Sapoval, B., 2004. An optimal bronchial tree may be dangerous. Nature 427, 633–636.

Meier-Ruge, W., Ulrich, J., Bruhlmann, M., Meier, E., 1992. Age-related white matter atrophy in the human brain. Ann. N. Y. Acad. Sci. 673, 260–269.

O'Leary, D.H., Polak, J.F., Kronmal, R.A., Manolio, T.A., Burke, G.L., Wolfson, S.K. Jr., 1999. Carotid-artery intima and media thickness as a risk factor for myocardial infarction and stroke in older adults. N. Engl. J. Med. 340, 14–22.

Pantoni, L., 2002. Pathophysiology of age-related cerebral white matter changes. Cerebrovasc. Dis. 13 (Suppl. 2), 7–10.

Pico, F., Dufouil, C., Levy, C., Besancon, V., de Kersaint-Gilly, A., Bonithon-Kopp, C., Ducimetiere, P., Tzourio, C., Alperovitch, A., 2002. Longitudinal study of carotid atherosclerosis and white matter hyperintensities: the EVA-MRI cohort. Cerebrovasc. Dis. 14, 109–115.

Pugh, K.G., Lipsitz, L.A., 2002. The microvascular frontal-subcortical syndrome of aging. Neurobiol. Aging 23, 421–431.

Salloway, S., Malloy, P., Kohn, R., Gillard, E., Duffy, J., Rogg, J., Tung, G., Richardson, E., Thomas, C., Westlake, R., 1996. MRI and neuropsychological differences in early- and late-life-onset geriatric depression. Neurology 46, 1567–1574.

Schmidt, R., Fazekas, F., Enzinger, C., Ropele, S., Kapeller, P., Schmidt, H., 2002. Risk factors and progression of small vessel disease-related cerebral abnormalities. J. Neural. Transm. Suppl. (62), 47–52.

Schmidt, R., Scheltens, P., Erkinjuntti, T., Pantoni, L., Markus, HS., Wallin, A., Barkhof, F., Fazekas, F., 2004. White matter lesion progression: a surrogate endpoint for trials in cerebral small-vessel disease. Neurology 63, 139–144.

Shimizu, Y., Barth, M., Windischberger, C., Moser, E., Thurner, S., 2004. Wavelet-based multifractal analysis of fMRI time series. NeuroImage 22, 1195–1202.

Stanley, H.E., Amaral, L.A., Goldberger, A.L., Havlin, S., Ivanov, P.Ch, Peng, C,K., 1999. Statistical physics and physiology, monofractal and multifractal approaches. Physica A 270, 309–324.

Takahashi, T., Murata, T., Omori, M., Kimura, H., Kado, H., Kosaka, H., Takahashi, K., Itoh, H., Wada, Y., 2001. Quantitative evaluation of magnetic resonance imaging of deep white matter hyperintensity in geriatric patients by multifractal analysis. Neurosci. Lett. 314, 143–146.

Takahashi, T., Murata, T., Omori, M., Kosaka, H., Takahashi, K., Yonekura, Y., Wada, Y., 2004. Quantitative evaluation of age-related white matter microstructural changes on MRI by multifractal analysis. J. Neurol. Sci. 225, 33–37.

Takao, M., Koto, A., Tanahashi, N., Fukuuchi, Y., Takagi, M., Morinaga, S., 1999. Pathologic findings of silent hyperintense white matter lesions on MRI. J. Neurol. Sci. 167, 127–131.

Touboul, P.J., Elbaz, A., Koller, C., Lucas, C., Adrai, V., Chedru, F. Amarenco P., 2000. Common carotid artery intima-media thickness and brain infarction: the Etude du Profil Genetique de l'Infarctus Cerebral (GENIC) case-control study. Circulation 102, 313–318.

Valenzuela, M.J., Sachdev, P.S., Wen, W., Shnier, R., Brodaty, H., Gillies, D., 2000. Dual voxel proton magnetic resonance spectroscopy in the healthy elderly, subcortical-frontal axonal N-acetylaspartate levels are correlated with fluid cognitive abilities independent of structural brain changes. NeuroImage 12, 747–756.

van Swieten, J.C., van den Hout, J.H., van Ketel, B.A., Hijdra, A., Wokke, J.H., van Gijn, J., 1991. Periventricular lesions in the white matter on magnetic resonance imaging in the elderly: a morphometric correlation with arteriolosclerosis and dilated perivascular spaces. Brain 114, 761–774.

Varma, A.R., Laitt, R., Lloyd, J.J., Carson, K.J., Snowden, J.S., Neary, D., Jackson, A., 2002. Diagnostic value of high signal abnormalities on T2 weighted MRI in the differentiation of Alzheimer's, frontotemporal and vascular dementias. Acta. Neurol. Scand. 105, 355–364.

Yamamoto, A., Miki, Y., Tomimoto, H., Kanagaki, M., Takahashi, T., Fushimi, Y., Konishi, J., Laz, Haque. T, Togashi, K., 2005. Age-related signal intensity changes in the corpus callosum, assessment with three orthogonal FLAIR images. Eur. Radiol. 15, 2304–2311.

Ylikoski, R., Ylikoski, A., Erkinjuntti, T., Sulkava, R., Raininko, R., Tilvis, R., 1993. White matter changes in healthy elderly persons correlate with attention and speed of mental processing. Arch. Neurol. 50, 818–824.

Yoshikawa, T., Murase, K., Oku, N., Imaizumi, M., Takasawa, M., Rishu, P., Kimura, Y., Ikejiri, Y., Kitagawa, K., Hori, M., Hatazawa, J., 2003a. Heterogeneity of cerebral blood flow in Alzheimer disease and vascular dementia. AJNR Am. J. Neuroradiol. 24, 1341–1347.

Yoshikawa, T., Murase, K., Oku, N., Kitagawa, K., Imaizumi, M., Takasawa, M., Nishikawa, T., Matsumoto, M., Hatazawa, J., Hori, M., 2003b. Statistical image analysis of cerebral blood flow in vascular dementia with small-vessel disease. J. Nucl. Med. 44, 505–511.

Zamir M., 1999. On fractal properties of arterial trees. J. Theor. Biol. 197, 517–526.

Zureik, M., Touboul, P.J., Bonithon-Kopp, C., Courbon, D., Berr, C., Leroux, C., Ducimetiere, P., 1999. Cross-sectional and 4-year longitudinal associations between brachial pulse pressure and common carotid intima-media thickness in a general population: the EVA study. Stroke 30, 550–555.

Figure legends

Fig. 1. Typical example of $f(\alpha)$ spectrum in a deep white matter ROI. The slope at each plot of the smooth concave function shows the q value. The $\alpha(q)$ value at $q = -20$ was defined as α_{max} (right end of the $f(\alpha)$ spectrum), while the $\alpha(q)$ value at $q = +20$ was defined as α_{min} (left end of the $f(\alpha)$ spectrum). The width of both ends of the $f(\alpha)$ spectrum was defined as $\Delta\alpha$.

Fig. 2. Representative sagittal (A) and axial (B) slices from T2-weighted MR images demonstrate ROI placement. A rectangular $x \times y$ pixel ROI ($1600 < x \times y < 2000$; $x, y >$ 32 pixels) was placed bilaterally in the deep white matter of the frontoparietal region in the vicinity of the lateral ventricles (white line on A and white rectangle on B). ROIs were chosen manually to avoid including the cortex, the ventricles, and abnormal white matter intensities. The rectangular $x \times y$ pixel ROI consisted of $(x - 32 + 1) \times (y - 32 + 1)$ frames of 32 × 32 pixel images. A typical example of the rectangular regions of interest (ROIs: 38 × 48 pixels) on T2-weighted MR images selected from the deep white matter of the frontoparietal region (B) and MR signal intensity fluctuations in the ROI (C, with magnification). Fig. 2D shows divided images with sides of $r = 1, 2, 4, 8, 16$, and 32 pixels.

Fig. 3. Examples of simulated homogeneous images such as simple gray (A), standard fractal objects such as Sierpinski's gaskets (B1–3 from homogeneous to heterogeneous type), randomized noise (C), and averaged image of 10 ROIs with DWMH (D). Figs. E1 and E2 show images of selected ROIs with high and low $\Delta\alpha$. In Fig. F, lines represent

theoretical values and dots show actual values. Red dots demonstrate the theoretical and actual values of a simple Sierpinski's gasket (B_1). The green line and dots show results for the heterogeneous Sierpinski's gasket (B_2). The blue line and dots show the results for a more heterogeneous Sierpinski's gasket (B_3). With increasing heterogeneity of the image (from B_1 to B_3), the width of both ends of α gradually increases (as shown in F).

Fig. 4. Association between $\Delta\alpha$ and intima-media thickness (IMT). Significant positive correlations were observed (all subjects (open and closed circles): $r = 0.515$, $P < 0.001$; subjects without DWMH (closed circles): $r = 0.540$, $P = 0.006$) for the right side (A). Significant positive correlations were observed (all subjects (open and closed circles): $r = 0.472$, $P = 0.004$; subjects without DWMH (closed circles): $r = 0.610$, $P = 0.002$) for the left side (B).

Fig. 5. $\Delta\alpha$ values across intima-media thickness (IMT) groups (high- vs. low-IMT), right and left sides, respectively. Values are mean ± SD. *$P < 0.05$ (ANCOVA).

Figure 1 in TIFF format

Click here to download high resolution image

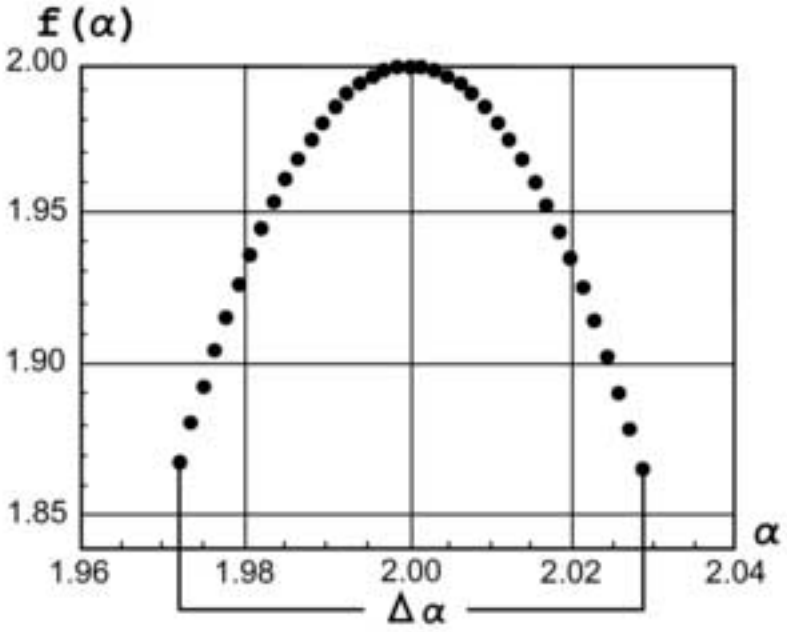

Figure 2 in TIFF format
Click here to download high resolution image

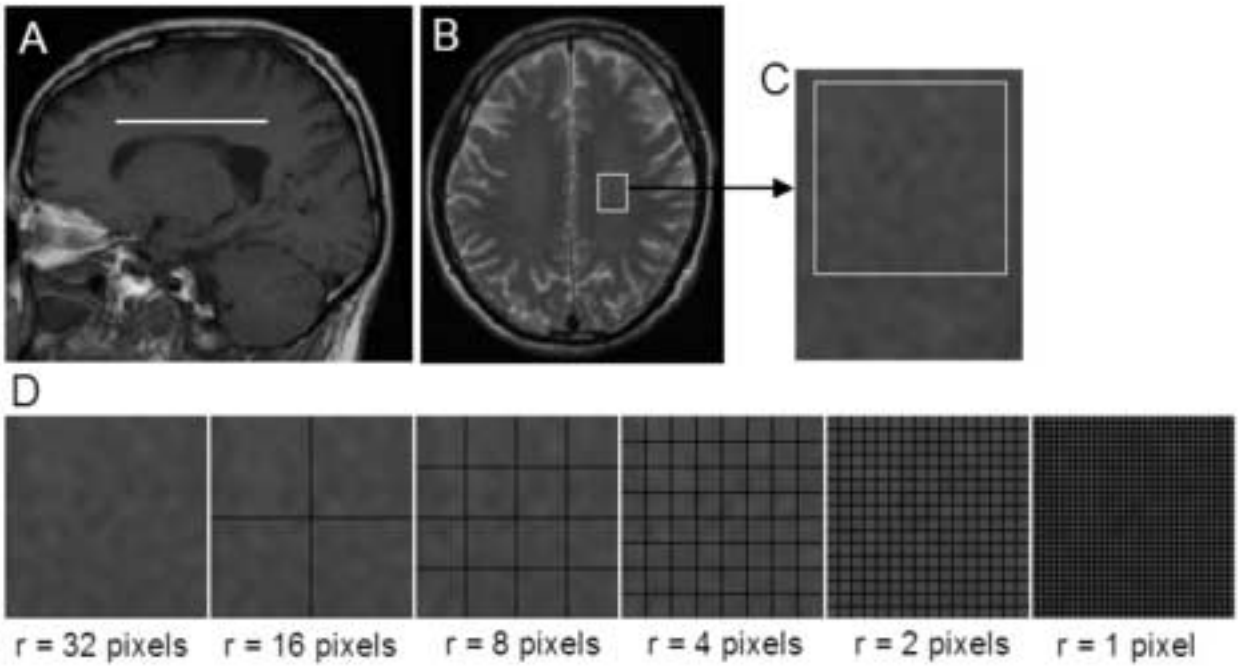

Figure 3 in TIFF format
Click here to download high resolution image

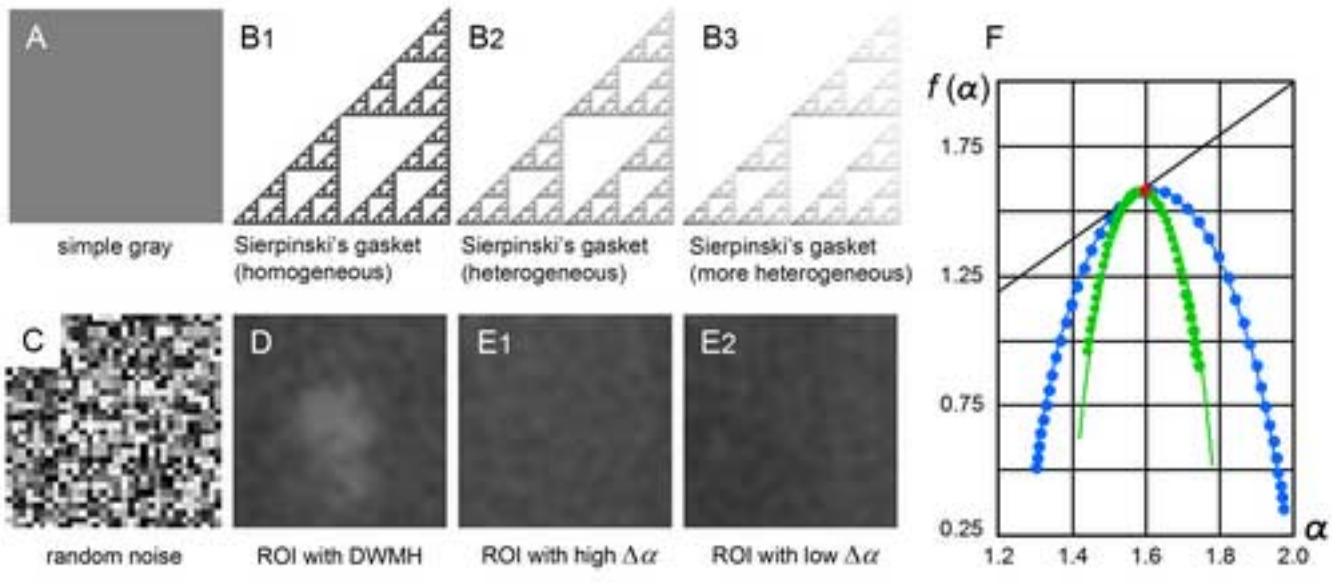

Figure 4 in TIFF format
Click here to download high resolution image

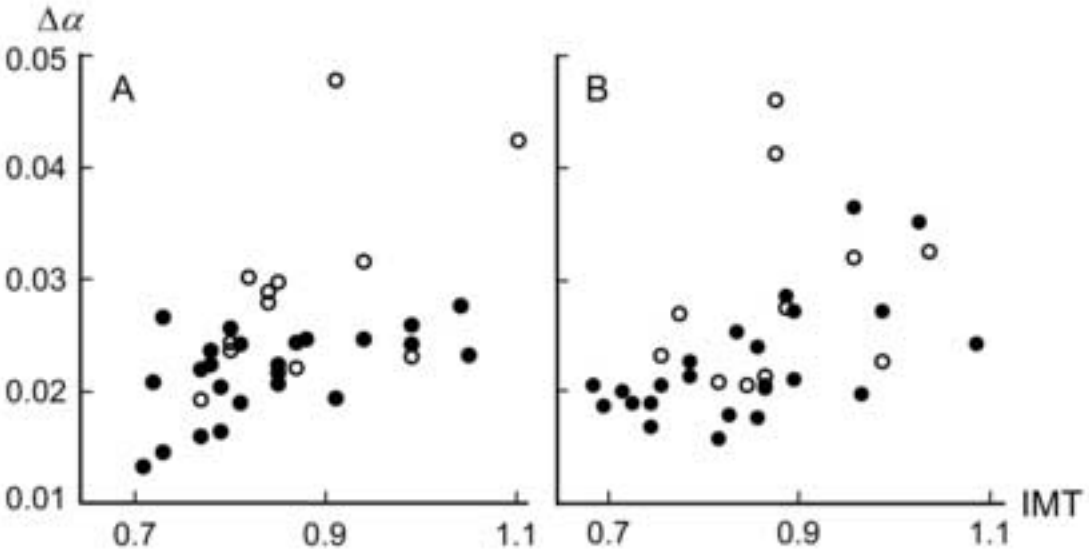

Figure 5 in TIFF format
Click here to download high resolution image

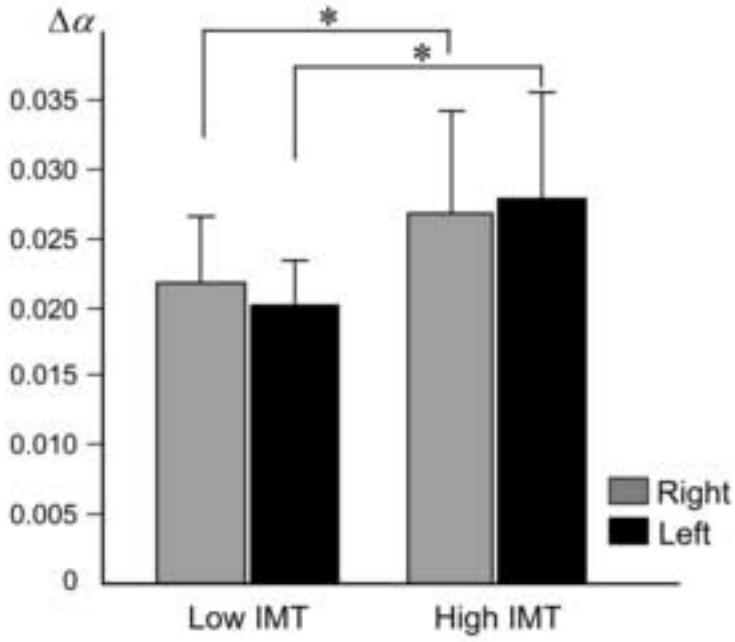

Table 1

Table 1
Demographic characteristics of the study subjects with comparison between gender groups

	Male (n = 23)	Female (n = 13)	*P*
Right $\Delta\alpha$, mean (SD)	0.0246 (0.0062)	0.0237 (0.0077)	0.725
Left $\Delta\alpha$, mean (SD)	0.0251 (0.0078)	0.0219 (0.0046)	0.181
Right SD/MSI, mean (SD)	0.0347 (0.0071)	0.0275 (0.0046)	0.002**
Left SD/MSI, mean (SD)	0.0340 (0.0071)	0.0274 (0.0036)	0.004**
Right IMT (mm), mean (SD)	0.863 (0.090)	0.838 (0.112)	0.463
Left IMT (mm), mean (SD)	0.868 (0.096)	0.843 (0.110)	0.479
Age (years), mean (SD)	60.96 (4.74)	60.85 (4.10)	0.944
BMI (kg/m^2), mean (SD)	23.90 (2.01)	22.43 (2.65)	0.069
TC (mg/dl), mean (SD)	200.95 (31.59)	227.00 (37.03)	0.032*
SBP (mm Hg), mean (SD)	126.35 (13.56)	119.15 (11.00)	0.112
Co-existence of DWMH (%), (n)	30.4 (7/23)	30.8 (4/13)	0.635

Data are expressed as mean ± S.D.; SD/MSI, standard deviation of signal intensity divided by mean value of signal intensity; IMT, intima-media thickness; BMI, body mass index; TC, total cholesterol; SBP, systolic blood pressure; DWMH, deep white matter hyperintensity. *$P < 0.05$; ** $P < 0.01$.

Table 2

Table 2

Correlation matrix of $\Delta\alpha$, SD/MSI, IMT, age, BMI, TC, and systolic BP in all subjects

Right side	Right SD/MSI	Right IMT	Age	BMI	TC	SBP
Right $\Delta\alpha$	0.624**	0.515**	0.109	-0.075	0.101	0.001
Right SD/MSI	-	0.397*	-0.119	0.342*	0.232	-0.100
Right IMT (mm)	-	-	0.206	0.193	-0.064	0.183
Left side	**Left SD/MSI**	**Left IMT**	**Age**	**BMI**	**TC**	**SBP**
Left $\Delta\alpha$	0.618**	0.474**	-0.091	0.106	0.015	0.127
Left SD/MSI	-	0.222	0.163	0.347*	0.268	-0.128
Left IMT (mm)	-	-	0.324	0.312	0.051	0.226

Correlation matrix among confounding factors

	BMI	TC	SBP
Age (years)	-0.032	0.128	-0.033
BMI (kg/m^2)	-	-0.066	0.367*
TC (mg/dl)	-	-	-0.121

SD/MSI, standard deviation of signal intensity divided by mean value of signal intensity; IMT, intima-media thickness; BMI, body mass index; TC, total cholesterol; SBP, systolic blood pressure; DWMH, deep white matter hyperintensity. *$P < 0.05$; ** $P < 0.01$.

Table 3

Table 3
Summary of multiple linear regression analysis for right and left IMT with $\Delta\alpha$

Right side	All subjects		Subjects without DWMH	
	β	P	β	P
Right $\Delta\alpha$	0.514	0.001	0.478	0.017
Age (years)	0.157	0.293	0.038	0.828
Gender (%)	-0.148	0.883	-0.179	0.355
BMI (kg/m^2)	0.149	0.145	0.338	0.071

Left side	All subjects		Subjects without DWMH	
	β	P	β	P
Left $\Delta\alpha$	0.497	0.001	0.635	0.001
Age (years)	0.380	0.008	0.359	0.025
Gender (%)	0.087	0.549	0.077	0.622
BMI (kg/m^2)	0.298	0.043	0.277	0.083

IMT, intima-media thickness; BMI, body mass index; DWMH, deep white matter hyperintensity. β is the standardized regression coefficient, which allows comparison of the relative contribution of each variable to the prediction of IMT. For this model, multiple $r = 0.587$, $r^2 = 0.344$, $P = 0.009$ (for all subjects); $r = 0.686$, $r^2 = 0.471$, $P = 0.013$ (for subjects without DWMH) for right side and multiple $r = 0.664$, $r^2 = 0.441$, $P < 0.001$ (for all subjects); $r = 0.779$, $r^2 = 0.606$, $P < 0.001$ (for subjects without DWMH) for left side, respectively.

Table 4

Table 4
Summary of multiple linear regression analysis for right and left IMT with SD/MSI

Right side	All subjects		Subjects without DWMH	
	β	P	β	P
Right SD/MSI	0.465	0.018	0.461	0.067
Age (years)	0.265	0.104	0.122	0.519
Gender (%)	0.131	0.479	-0.161	0.462
BMI (kg/m^2)	0.082	0.630	0.105	0.617

Left side	All subjects		Subjects without DWMH	
	β	P	β	P
Left SD/MSI	0.222	0.239	0.227	0.363
Age (years)	0.370	0.027	0.324	0.130
Gender (%)	0.069	0.706	-0.005	0.981
BMI (kg/m^2)	0.268	0.124	0.234	0.305

SD/MSI, standard deviation of signal intensity divided by mean value of signal intensity; IMT, intima-media thickness; BMI, body mass index; DWMH, deep white matter hyperintensity. β is the standardized regression coefficient, which allows comparison of the relative contribution of each variable to the prediction of IMT. For this model, multiple $r = 0.489$, $r^2 = 0.239$, $P = 0.069$ (for all subjects); $r = 0.632$, $r^2 = 0.400$, $P = 0.038$ (for subjects without DWMH) for right side and multiple $r = 0.494$, $r^2 = 0.244$, $P = 0.062$ (for all subjects); $r = 0.524$, $r^2 = 0.274$, $P = 0.171$ (for subjects without DWMH) for left side, respectively.

Table 5

Table 5
Correlation matrix of $\Delta\alpha$, SD/MSI, IMT, age, BMI, TC, and systolic BP in subjects without DWMH

Right side	Right SD/MSI	Right IMT	Age	BMI	TC	SBP
Right $\Delta\alpha$	0.592**	0.540**	0.017	-0.024	-0.345	0.071
Right SD/MSI	-	0.589**	-0.064	0.453*	-0.273	0.084
Right IMT (mm)	-	-	0.128	0.377	-0.215	0.225

Leftt side	Left SD/MSI	Left IMT	Age	BMI	TC	SBP
Left $\Delta\alpha$	0.454**	0.610**	-0.087	0.100	0.023	0.002
Left SD/MSI	-	0.299	-0.083	0.412*	-0.235	0.011
Left IMT (mm)	-	-	0.352	0.392	0.039	0.226

Correlation matrix among confounding factors

	BMI	TC	SBP
Age (years)	0.197	0.192	0.127
BMI (kg/m^2)	-	-0.058	0.231
TC (mg/dl)	-	-	-0.304

SD/MSI, standard deviation of signal intensity divided by mean value of signal intensity; IMT, intima-media thickness; BMI, body mass index; TC, total cholesterol; SBP, systolic blood pressure; DWMH, deep white matter hyperintensity.
*$P < 0.05$; ** $P < 0.01$.